Cell

A functional cellular framework for sex and estrous cycle-dependent gene expression and behavior

Graphical abstract

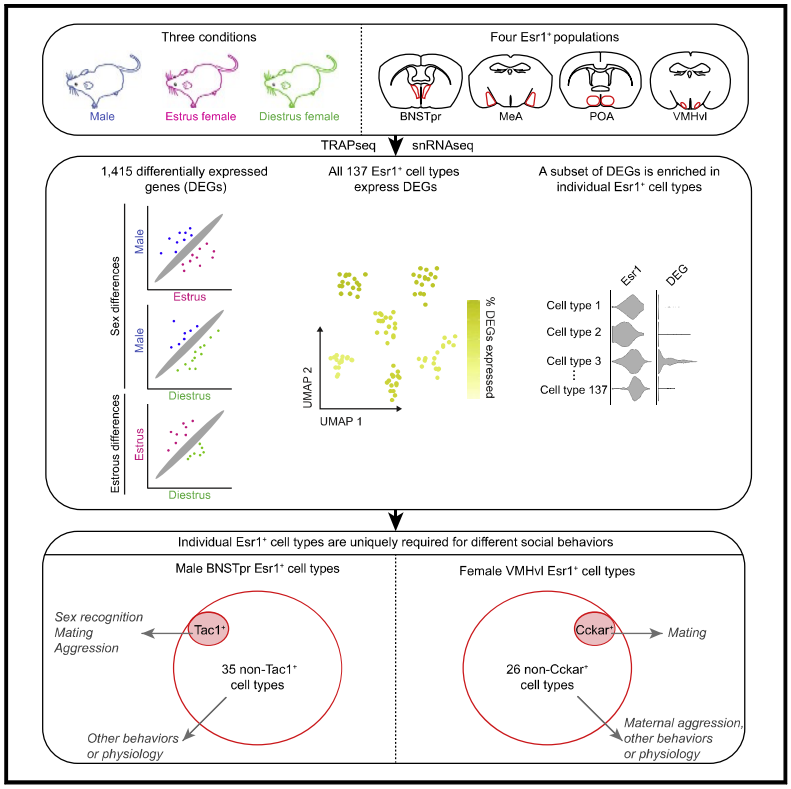

Highlights

- 1,415 genes are dimorphic by sex or estrous state in four Esr1$^+$ neuronal populations
- All 137 Esr1$^+$ cell types within these four populations express subsets of these genes
- Only 1 male BNSTpr Esr1$^+$ cell type is needed to recognize sexes, mate, and fight
- Only 1 female VMHvl Esr1$^+$ cell type has dynamic projections and is needed to mate

Authors

Joseph R. Knoedler, Sayaka Inoue, Daniel W. Bayless, ..., Charu Ramakrishnan, Karl Deisseroth, Nirao M. Shah

Correspondence

nirao@stanford.edu

In brief

Differentially expressed genes in four estrogen receptor 1-expressing populations in different sexes or estrous states are identified along with a functional characterization of specific cell types that mediate social behaviors in male or female mice.

Knoedler et al., 2022, Cell *185*, 1–18
February 17, 2022
https://doi.org/10.1016/j.cell.2021.12.031

CellPress

Cell

CellPress

Article

A functional cellular framework for sex and estrous cycle-dependent gene expression and behavior

Joseph R. Knoedler,[1] Sayaka Inoue,[1,8] Daniel W. Bayless,[1,8] Taehong Yang,[1,8] Adarsh Tantry,[1,8] Chung-ha Davis,[4] Nicole Y. Leung,[1] Srinivas Parthasarathy,[6] Grace Wang,[1] Maricruz Alvarado,[1] Abbas H. Rizvi,[7] Lief E. Fenno,[1] Charu Ramakrishnan,[5] Karl Deisseroth,[1,3] and Nirao M. Shah[1,2,9,*]

[1]Department of Psychiatry and Behavioral Sciences, Stanford University, Stanford, CA 94305, USA
[2]Department of Neurobiology, Stanford University, Stanford, CA 94305, USA
[3]Department of Bioengineering, Stanford University, Stanford, CA 94305, USA
[4]Neurosciences Graduate Program, Stanford University, Stanford, CA 94305, USA
[5]CNC Program, Stanford University, Stanford, CA 94305, USA
[6]Accent Therapeutics, 65 Hayden Avenue, Lexington, MA 02421, USA
[7]Zuckerman Mind Brain Behavior Institute, Columbia University, New York, NY 10027, USA
[8]These authors contributed equally
[9]Lead contact
*Correspondence: nirao@stanford.edu
https://doi.org/10.1016/j.cell.2021.12.031

SUMMARY

Sex hormones exert a profound influence on gendered behaviors. How individual sex hormone-responsive neuronal populations regulate diverse sex-typical behaviors is unclear. We performed orthogonal, genetically targeted sequencing of four estrogen receptor 1-expressing (Esr1$^+$) populations and identified 1,415 genes expressed differentially between sexes or estrous states. Unique subsets of these genes were distributed across all 137 transcriptomically defined Esr1$^+$ cell types, including estrous stage-specific ones, that comprise the four populations. We used differentially expressed genes labeling single Esr1$^+$ cell types as entry points to functionally characterize two such cell types, BNSTpr$^{Tac1/Esr1}$ and VMHvl$^{Cckar/Esr1}$. We observed that these two cell types, but not the other Esr1$^+$ cell types in these populations, are essential for sex recognition in males and mating in females, respectively. Furthermore, VMHvl$^{Cckar/Esr1}$ cell type projections are distinct from those of other VMHvl^{Esr1} cell types. Together, projection and functional specialization of dimorphic cell types enables sex hormone-responsive populations to regulate diverse social behaviors.

INTRODUCTION

In many vertebrates, neural circuits underlying sex or estrous (menstrual) state-typical physiology and social behaviors are regulated by sex hormones (Arnold, 2009; Beeman, 1947; Brock et al., 2011; Dey et al., 2015; Honda et al., 1998; Inoue et al., 2019; Juntti et al., 2010; Kow and Pfaff, 1998; Musatov et al., 2006; Ogawa et al., 2000; Phoenix et al., 1959; Ring, 1944; Rissman et al., 1997; Scordalakes and Rissman, 2003; Shapiro, 1937; Toda et al., 2001; Wu et al., 2009; Yang and Shah, 2014). There has been significant progress in delineating sex hormone-responsive populations that govern such state-specific physiology and behavior. In particular, neurons in the principal component of the bed nucleus of the stria terminalis (BNSTpr), medial amygdala (MeA), preoptic hypothalamus (POA), and ventromedial hypothalamus ventrolateralis (VMHvl) have been shown to regulate sex or estrous state-dependent displays of mating and aggression (Bayless et al., 2019; Hashikawa et al., 2017; Hong et al., 2014; Ishii et al., 2017; Karigo et al., 2021; Lee et al., 2014; Lin et al., 2011; Musatov et al., 2006; Osakada et al., 2018; Unger et al., 2015; Wei et al., 2018; Yang et al., 2013, 2017; Yao et al., 2017). Surprisingly, each of these regions regulates multiple such behaviors or physiological responses. How this diversity of function is implemented within individual sex hormone-responsive populations is an open question.

Sex or estrous state-typical gene expression could endow subsets of neurons with distinct functional properties within the BNSTpr, MeA, POA, and VMHvl to drive multiple outputs. However, recent studies of these regions have uncovered many transcriptomically defined cell types (cell types, hereafter) but few or no sex or estrous state-dependent gene expression differences in these cell types (Chen et al., 2019; Kim et al., 2019; Moffitt et al., 2018; Welch et al., 2019; Xu et al., 2012). These findings immediately raise the question as to how such cell types generate sex or estrous stage-dependent functional outputs. It

Please cite this article in press as: Knoedler et al., A functional cellular framework for sex and estrous cycle-dependent gene expression and behavior, Cell (2022), https://doi.org/10.1016/j.cell.2021.12.031

is possible that the small number of gene expression differences between sexes or estrous states is sufficient to functionally diversify individual regions to drive multiple sex hormone-dependent outputs. Alternatively, prior efforts have underestimated the number of differentially expressed genes (DEGs) because they did not enrich for sex hormone-sensitive neurons. This is a nontrivial possibility because only a subset of neurons expresses sex hormone receptors in these regions, leading to under-sampling of the relevant neurons.

In order to distinguish between these possibilities, we wished to first identify DEGs between sexes (sDEGs) using a high throughput sequencing approach that affords deep and reliable coverage of sex hormone-sensitive neurons. We reasoned that if this yielded many sDEGs, we would use single cell RNA sequencing to map their distribution within the individual cell types that comprise sex hormone-sensitive populations. Esr1 (or ERα) is essential for sex-typical behaviors in both sexes and expressed in subsets of neurons within the BNSTpr (BNSTpr^{Esr1}), POA (POA^{Esr1}), MeA (MeA^{Esr1}), and VMHvl (VMHvl^{Esr1}) (Kim et al., 2019; Ogawa et al., 2000; Paxinos and Franklin, 2003; Rissman et al., 1997; Scordalakes and Rissman, 2003; Wu and Tollkuhn, 2017; Xu et al., 2012; Yang et al., 2013). To identify sDEGs in these four estrogen receptor 1-expressing (Esr1$^+$) populations, we performed translating ribosome affinity purification and sequencing (TRAPseq) (Heiman et al., 2008; Sanz et al., 2009), which enabled rapid mRNA extraction and deep, reliable coverage of translated mRNAs. Having identified numerous DEGs, we sought to define their distribution within these Esr1$^+$ populations with single-nucleus RNA sequencing (snRNA-seq), using a modified INTACT approach (Mo et al., 2015).

We profiled Esr1$^+$ neurons from females modeled to be in two distinct stages of the estrous cycle, estrus and diestrus (Ring, 1944). Estrus and diestrus states reflect changes in circulating estrogen and progesterone with corresponding maxima and minima of sexual behavior. We reasoned that our approach would enable discovery of sDEGs that differ between females in distinct estrous states and males; in addition, it would reveal any potential DEGs that differ between these two estrous states (eDEGs).

We have identified 1,415 DEGs between sexes or estrous stages. Unique subsets of these DEGs are distributed across all 137 cell types that comprise the four Esr1$^+$ populations we surveyed. Such diversification of gene expression between sexes and estrous states provides potential mechanisms whereby individual Esr1$^+$ populations influence multiple gendered behaviors. We used such DEGs to genetically access individual Esr1$^+$ cell types and developed an intersectional genetic approach to assess behavioral functions of single cell types and their complementary counterparts. For each Esr1$^+$ cell type we manipulated, we observed a restricted contribution to sex or estrous state-dependent social interactions that was distinct from that of the other Esr1$^+$ cell types in that region. Together, our findings reveal a large diversity of sexually differentiated and estrous state-dependent cell types in the mammalian brain. The modular contribution to gendered behaviors of the cell types that we have characterized provides a mechanism whereby individual sex hormone-responsive populations regulate diverse behaviors. Such partitioning of behavioral functions to different cell types within a population may be a general feature of the many transcriptomically defined cell types that have been identified throughout the brain.

RESULTS

Identification of sex-differential gene expression

Adult males maintain testosterone at a steady state and reliably initiate sex hormone-dependent social behaviors whereas females exhibit cyclic changes in sex hormone titers, with peak titers at estrus opening a window of sexual receptivity. Such cyclic changes in gene expression can confound sDEG identification, and we therefore collected tissue from estrus and diestrus females. We generated sexually receptive estrus (F_R) mice with estrogen and progesterone priming and diestrus sexually non-receptive (F_{NR}) mice with vehicle priming (Figure S1A). Our protocol for F_R and F_{NR} mice both mimics estrogen and progesterone titers corresponding to natural estrus and diestrus and recapitulates these cycle stages behaviorally: F_R mice are sexually receptive like estrus females, and F_{NR} mice are non-receptive like diestrus females (Inoue et al., 2019; Ring, 1944).

We performed TRAPseq on BNSTpr, MeA, POA, and VMHvl from adult F_R, F_{NR}, and gonadally intact male (M) mice bearing an *Esr1^{Cre}* and a Cre-dependent allele (*Rpl22^{HA}*) encoding an HA-tagged ribosomal subunit (Figures 1A, S1B, and S1C; Table S1) (Lee et al., 2014; Sanz et al., 2009). In order to identify sDEGs (M v F_R and M v F_{NR} comparisons; v, versus), we employed a negative binomial model for RNA-seq data analysis (DESeq2) (Love et al., 2014), focusing on DEGs that exhibited $\geq$1.5-fold change and passed a false discovery rate (FDR) criterion of <0.05. This revealed 1,541 differential gene expression events between sexes (890 sDEGs, M v F_R; 651 sDEGs, M v F_{NR}) (Figure 1B; Table S2). We identified numerous female upregulated sDEGs, even in regions such as the BNSTpr and POA in which males have more neurons, thereby validating the sensitivity of our approach (Figure S1E; Table S2). sDEG-encoding loci reside on all chromosomes, and many sDEGs appear insensitive to estrous cycle state (Figures S1D and S1E), in that they are differentially expressed between males and females irrespective of hormone priming. We next used hybridization chain reaction based *in situ* hybridization (ISH) to visualize sDEGs spanning a range of expression levels (1–220 transcripts per million) and fold changes (1.5–15) (Figures 1C and S1F) (Choi et al., 2018). Our studies confirmed differential expression for all 23 sDEGs that we had selected for *in vivo* analysis (Figures 1C and S1F; data not shown). Together, we have uncovered large-scale, genome-wide regulation of gene expression by sex.

Identification of estrous cycle stage-differential gene expression

Even for regions such as the BNSTpr, MeA, POA, and VMHvl that regulate female behaviors, prior gene expression profiling studies have not compared males with females in distinct estrous stages in naturally cycling or F_R and F_{NR} mice (Chen et al., 2019; Kim et al., 2019; Moffitt et al., 2018; Welch et al., 2019; Xu et al., 2012). We analyzed our dataset for eDEGs, or genes that differed significantly in expression between F_R and

Please cite this article in press as: Knoedler et al., A functional cellular framework for sex and estrous cycle-dependent gene expression and behavior, Cell (2022), https://doi.org/10.1016/j.cell.2021.12.031

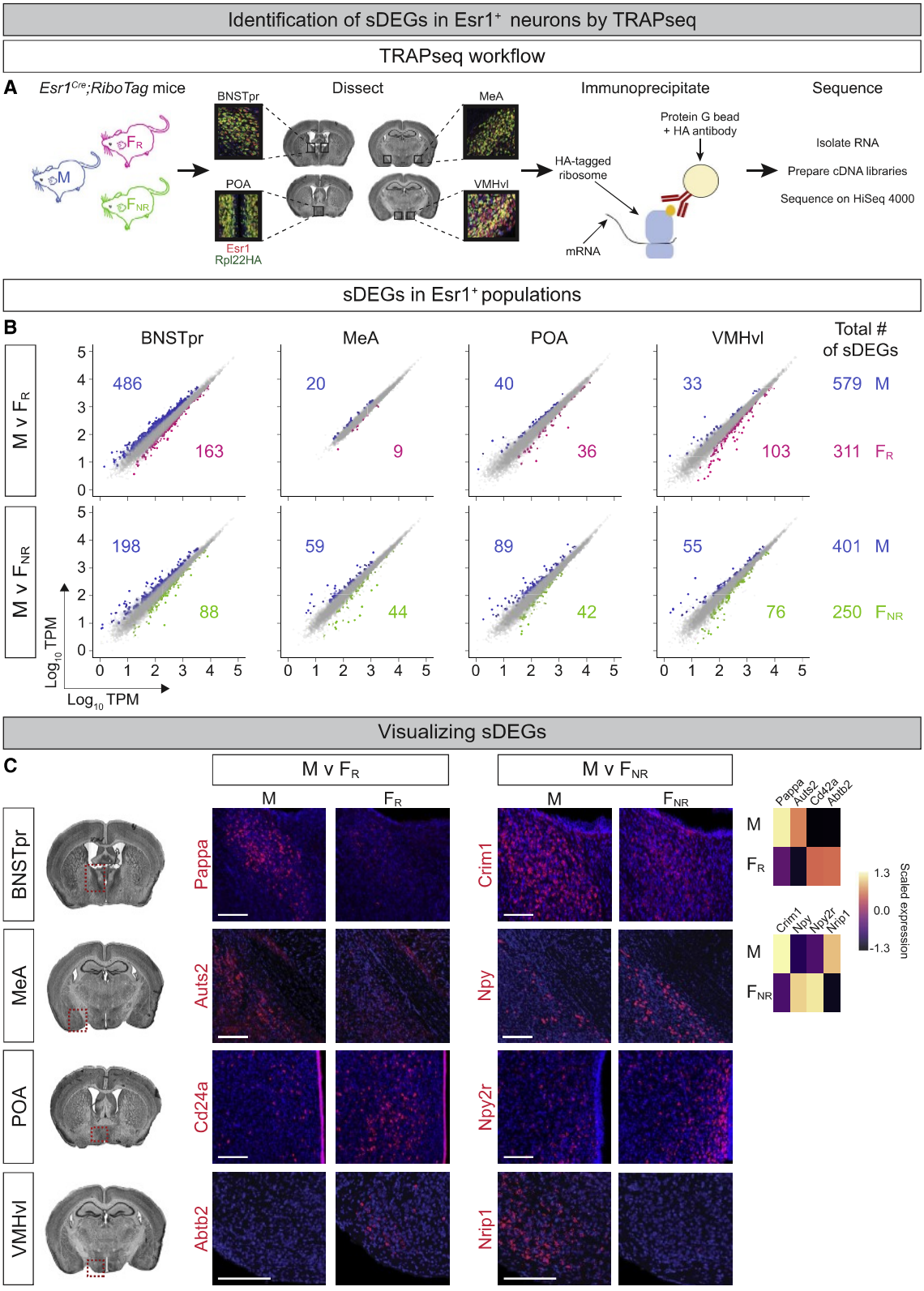

(legend on next page)

Please cite this article in press as: Knoedler et al., A functional cellular framework for sex and estrous cycle-dependent gene expression and behavior, Cell (2022), https://doi.org/10.1016/j.cell.2021.12.031

F_{NR} mice. We identified 770 such differential expression events using inclusion criteria we used for sDEGs (Figure 2A). Similar to sDEGs, eDEG-encoding loci reside on all chromosomes (Figure S2A). Our ISH studies confirmed differential expression for all eDEGs (n = 12 eDEGs) that we had selected for *in vivo* analysis (Figures 2B and S2B). Esr1 and progesterone receptor (PR) typically upregulate gene expression through recruitment of coactivator complexes (Ellmann et al., 2009; Green and Carroll, 2007). Nevertheless, a large fraction of eDEGs was upregulated in F_{NR} mice, suggesting de-repression as a mode of gene regulation in these Esr1$^+$ neurons. Irrespective of underlying mechanisms, our data reveal large-scale genome-wide regulation of gene expression by estrous state in multiple brain regions.

General properties of genes differentially expressed between sexes or estrous stages

Many DEGs are both sDEGs and eDEGs, such that 1,415 unique genes are differentially expressed between sexes or estrous states (Table S2). Each Esr1$^+$ population expresses a unique complement of DEGs, with only a subset of DEGs common to >2 regions (Figure 2C; Tables S2 and S3). Within individual Esr1$^+$ populations, most DEGs are unique to M v F_R, M v F_{NR}, or F_R v F_{NR} comparisons (Figure 2D; Table S3). Accordingly, principal component analysis (PCA) of DEGs within each region shows that M, F_R, and F_{NR} occupy distinct regions in PCA space, suggesting that F_R and F_{NR} mice are different from each other even in comparison to males (Figure S2C). DEG-encoding loci are significantly enriched for sex hormone receptor binding DNA elements, suggesting a shared transcriptional regulatory framework underlying these expression patterns (Figure S3A).

Gene Ontology analyses revealed a significant enrichment of DEGs in synaptic transmission, steroid hormone-related processes, behavior, peripheral reproductive organ processes, and regulation of gene expression (Figure S3B; Table S4) (Ashburner et al., 2000; Gene Ontology Consortium, 2021). These DEGs are not particularly enriched in developmental processes, consistent with the fact that TRAPseq was done on adult neurons. There are sex biases in many diseases, and we wondered if these DEGs were associated with such illnesses. A Disease Ontology analysis revealed enrichment for association with diverse sex-biased disorders, including autism spectrum disorder (ASD) (Figure S3C; Table S4) (Schriml et al., 2019). Many associations were for diseases affecting non-neural tissues, suggesting that these DEGs are also differentially expressed peripherally.

ASD is extremely sex-biased (male:female:: 4:1), and many genes have been identified as risk conferring with high confidence (Abrahams et al., 2013; Werling and Geschwind, 2013). Moreover, deficits in fundamental social interactions are a core feature of ASD. The four Esr1$^+$ populations we surveyed are critical for social behaviors, and we therefore examined potential associations between DEGs and high confidence ASD risk-conferring genes. We found that a significant number of such genes are DEGs in the adult mouse brain (39/207; $p = 3 \times 10^{-5}$) (Figure 3A) (Abrahams et al., 2013). We could also visualize differential expression of ASD risk-conferring DEGs *in vivo* with ISH (Figures 1C and 3B). Together, our findings suggest the possibility that ASD risk-conferring DEGs may contribute to disease-relevant behavioral domains by influencing Esr1$^+$ telencephalic as well as diencephalic neural pathways.

Identification of cell types that constitute the four Esr1$^+$ populations

Our ISH studies showed broad or restricted expression of DEGs within individual Esr1$^+$ populations (Figures 1C, 2B, S1F, and S2B). Dual-color ISH indeed confirmed that individual DEGs are expressed in most or a few Esr1$^+$ cells (dense and sparse expression patterns in Figure 3C). These findings suggested considerable heterogeneity of cell types in the four Esr1$^+$ populations we surveyed. Accordingly, we sought to characterize the distribution of DEGs at cellular resolution with snRNA-seq of Esr1$^+$ neurons from BNSTpr, MeA, POA, and VMHvl of adult F_R, F_{NR}, and male mice. To this end, we utilized mice bearing *Esr1^{Cre}* and *SunTag* (*Sun1/sfGFP*, which encodes a nuclear-membrane-targeted fluorescent protein) alleles (Figures S4A–S4C) (Mo et al., 2015). We analyzed data from the 49,776 Esr1$^+$ neurons that passed quality control criteria (Table S5).

We pooled sequencing data from all conditions/region and employed unsupervised graph-based clustering with Seurat to classify 137 Esr1$^+$ cell types (Hafemeister and Satija, 2019). Each cell type (36, BNSTpr; 34, MeA; 40, POA; 27, VMHvl; median cell #/cell type = 304) was uniquely labeled with one or a few genes (Figures 4 and S4D; Table S6). Importantly, Esr1$^+$ cell type classification was essentially unchanged even if DEGs were excluded from the clustering pipeline (data not shown). We cross-validated our Esr1$^+$ cell type classification using additional approaches. We obtained similar clustering results without pooling data from all conditions/region, indicating that clustering was not skewed by any particular condition. Indeed, analysis of all Esr1$^+$ cell types combined revealed co-clustering by brain region rather than batch, sex, or estrous stage (Figure S4E). Subsampling and bootstrapping approaches further confirmed that Esr1$^+$ cell types were reproducibly identifiable (Table S5) (Tang et al., 2020). Finally, the cell types we have identified align with those previously reported for the adult BNSTpr, POA, MeA,

Figure 1. TRAPseq identification of sex differences in gene expression

(A) Schematic of TRAPseq workflow.

(B) Scatterplots of sDEGs in different Esr1$^+$ populations. Dots represent DEGs with >1.5-fold change and FDR-adjusted p value <0.05 (colored) or genes that did not meet both criteria (gray). Colored numbers show number of sDEGs upregulated in that condition and comparison for each region and (far right) for all regions combined. In total, TRAPseq identified 890 and 651 sDEGs in M v F_R and M v F_{NR} comparisons. v, versus; TPM, transcripts/million. n = 3/condition.

(C) ISH for sDEGs in coronal sections through regions enclosed within red dotted areas on Nissl-stained sections on left. ISHs confirm TRAPseq data showing higher expression of Pappa, Auts2, Crim1, and Nrip1 in M and other genes upregulated in F_R or F_{NR} mice. Heatmap at far right shows scaled expression of DEGs that were visualized by ISH. Scale = mean z-scored expression of DEGs centered at zero for individual comparisons between conditions (sex or estrous state) and regions; analogous heatmaps provided for ISH studies in all figures. Coronal plane as well as dorsoventral and mediolateral orientations preserved for histological panels in all figures. n = 2/condition/probe. Red, mRNA; blue, DAPI. Scale bars = 100 μm.

See also Figure S1.

Please cite this article in press as: Knoedler et al., A functional cellular framework for sex and estrous cycle-dependent gene expression and behavior, Cell (2022), https://doi.org/10.1016/j.cell.2021.12.031

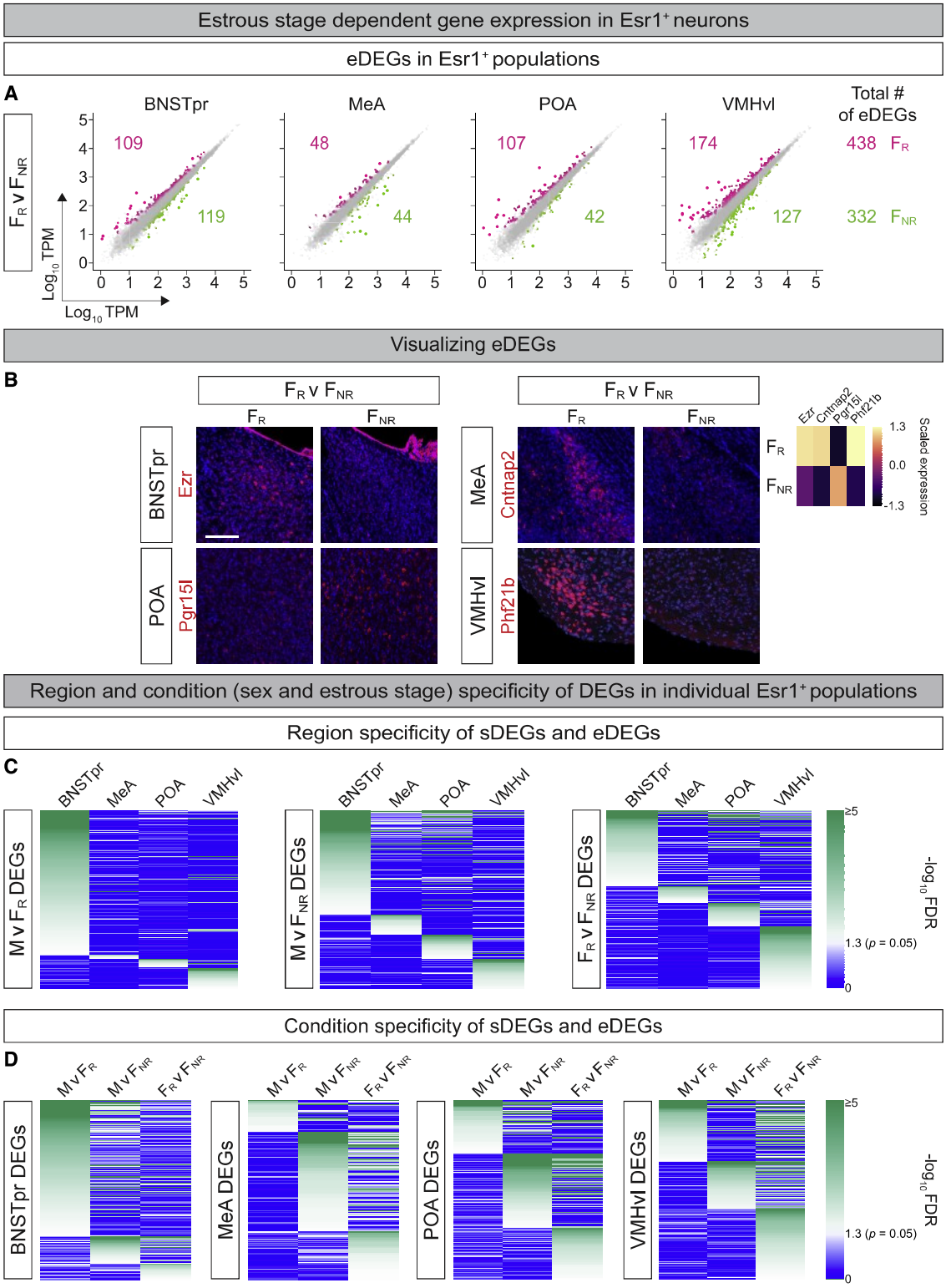

Figure 2. TRAPseq identification of estrous stage-dependent differences in gene expression

(A) Scatterplots of eDEGs in different Esr1+ populations. Dots represent DEGs with >1.5-fold change and FDR-adjusted p value <0.05 (colored) or genes that did not meet both criteria (gray). Colored numbers show number of eDEGs upregulated in that condition and comparison for each region and (far right) for all regions combined. In total, TRAPseq identified 770 eDEGs. n = 3.

(legend continued on next page)

Please cite this article in press as: Knoedler et al., A functional cellular framework for sex and estrous cycle-dependent gene expression and behavior, Cell (2022), https://doi.org/10.1016/j.cell.2021.12.031

and VMHvl using diverse sequencing platforms and analytical pipelines (Chen et al., 2019; Kim et al., 2019; Moffitt et al., 2018; Welch et al., 2019). As expected, absent from our dataset are Esr1$^-$ cell types identified by previous studies that performed single-cell/snRNA-seq without enriching for Esr1$^+$ populations. Sequencing purified Esr1$^+$ cells also allowed us to identify rare, biologically significant cell types or cell type-marker genes within the population. For example, we identified the Kiss1$^+$ cell type in POA, which is known to regulate ovulation and female mating (Hellier et al., 2018; Popa et al., 2008); we also identified aromatase$^+$ cell types in BNSTpr that are known to regulate sex recognition in males but were not assigned to this neuronal pool in a prior RNA-seq study that did not enrich for Esr1$^+$ cells (Figures 4A, 4C, and S4G) (Bayless et al., 2019; Welch et al., 2019).

All cell types we identified expressed canonical neuronal markers suggesting that most Esr1$^+$ cells in these regions are neurons (Figure S4G). Nearly all Esr1$^+$ cell types express PR and the androgen receptor (Figure 4), indicative of a broad influence of sex hormones on these populations. Most cell types in the BNSTpr and POA are inhibitory, whereas the MeA is composed of an equal mix of excitatory and inhibitory cell types (Figures 4A–4C and S4G). Although the VMHvl is largely glutamatergic, there is a small population of inhibitory neurons in this region (Figure S4F) (Lein et al., 2007). Consistent with this, we detected inhibitory Esr1$^+$ cell types in the VMHvl (Figures 4D and S4G).

We confirmed expression of ~98% of DEGs in our snRNA-seq data, in close concordance with the overall overlap (~95%) of the mRNAs between TRAPseq and snRNA-seq. Although in principle, DEGs could localize to one, a few, or most cell types, we observed DEGs in all cell types (Figures 5A–5D). Each cell type expressed ≥20% of DEGs, but none expressed the entire set of DEGs, and most DEGs were expressed in >1 cell type (Figures 5D and S5A). All Esr1$^+$ cell types harbored sDEGs and eDEGs. Although most harbored proportionally equivalent numbers of DEGs upregulated in M, F_R, or F_{NR} mice, a few were highly enriched for DEGs from one of these conditions (Figure 5E). This distribution of sDEGs and eDEGs was observed in excitatory as well as inhibitory cell types. While most DEGs were expressed in >1 cell type, many exhibited significant enrichment or depletion in ≥1 cell types, consistent with our ISH findings (Figures 3C and S5B).

We next tested whether individual cell types were differentially represented between M, F_R, and F_{NR} mice. We imposed stringent criteria, including a ≥3-fold cell number difference between ≥2 conditions as well as significant difference in relative abundance of cells, and identified 17 such cell types (Figure S5C). Most of these cell types occur in all conditions. However, the Cckar$^+$ cell type in the VMHvl (VMHvl$^{Cckar/Esr1}$) and the VMHvl$^{Trim36/Esr1}$ (expressing the eDEG *Trim36*) cell type appeared to be restricted to F_R and F_{NR} mice, respectively. A previous report identified the VMHvl$^{Cckar/Esr1}$ cell type, albeit annotated with *Tsix* and not assigned to the estrus phase, but not the VMHvl$^{Trim36/Esr1}$ cell type because VMHvl cells from F_{NR} mice were not profiled (Kim et al., 2019). It is possible that sequencing with higher depth of coverage will reveal additional condition-biased cell types. In any event, our current approach reveals several sex or estrous state-biased cell types and two that appear unique to F_R or F_{NR} mice.

The BNSTpr$^{Tac1/Esr1}$ cell type mediates the exclusively male requirement for aromatase$^+$ BNSTpr neurons in social behaviors

We sought to determine the behavioral role of single cell types in relation to the other Esr1$^+$ cell types in the population. Within the BNSTpr^{Esr1} population, the sex-shared BNSTpr$^{Tac1/Esr1}$ cell type is GABAergic and displays the highest enrichment for DEGs, with most DEGs upregulated in M compared to F_R and F_{NR} (Figures 6A, S6A, and S6B; Table S7). This cell type is also one of seven enriched for aromatase expression (Figures 4A and S4G), and we showed previously that aromatase$^+$ BNSTpr neurons are critical for male, but not female, social behaviors (Bayless et al., 2019). In males, these neurons are essential for sex recognition and the ensuing display of mating with females and aggression toward males. By contrast, their female counterparts are not active during social interactions nor are they essential for mating or maternal displays.

Tac1, encoding the neuropeptide tachykinin 1 or substance P, is an sDEG that is upregulated in males and expressed in a salt-and-pepper fashion, with an expression bias for the dorsal BNSTpr (Figures 6A, 6B, S1F, and S6C; Table S7). Tac1 signaling has been implicated in urine preference or social behaviors in males in diverse taxa (Asahina et al., 2014; Berger et al., 2012; Halasz et al., 2009; Katsouni et al., 2009; Siegel et al., 1997). This suggests the possibility that the BNST$^{Tac1/Esr1}$ cell type, uniquely among all aromatase$^+$ cell types within the BNSTpr^{Esr1} population, is critical for male social interactions.

We tested the functional role of the BNSTpr$^{Tac1/Esr1}$ cell type in male social interactions. We delivered a virally encoded, Cre-dependent, inhibitory chemogenetic actuator (AAV-flex-DREADDi:mCherry; DREADDi, designer receptor exclusively activated by designer drug, inhibitory) to the BNSTpr of adult males (*Tac1-Cre* mice) bearing a Cre recombinase inserted in a gene-conserving manner into the *Tac1* locus (Figure 6C) (Harris et al., 2014). The vast majority of Tac1$^+$ neurons co-label for Esr1 in the BNSTpr (97% ± 2%; 1,066 neurons analyzed, n = 2 mice), and our strategy therefore affords specific manipulation of the BNSTpr$^{Tac1/Esr1}$ cell type. We first tested whether, like aromatase$^+$ BNSTpr neurons, activity of the BNSTpr$^{Tac1/Esr1}$ cell type is required to distinguish between the sexes. Mice use pheromones to recognize the sexes, and male mice show a clear preference for urine, a rich source of pheromones, from females

(B) ISH for eDEGs. ISHs confirm TRAPseq data showing higher expression of Pgr15l in F_{NR} and other genes upregulated in F_R mice. n = 2/condition/probe. Scale bars = 100 μm.
(C) Heatmap of p values of individual DEGs for the relevant pairwise comparison (with darker green colors indicating more significant p values), illustrating that most DEGs are restricted to one Esr1$^+$ population.
(D) Heatmap of p values of individual DEGs for the relevant pairwise comparison (with darker green colors indicating more significant p values), illustrating that most DEGs within an Esr1$^+$ population are specific to one comparison between sexes or estrous states.
See also Figure S2.

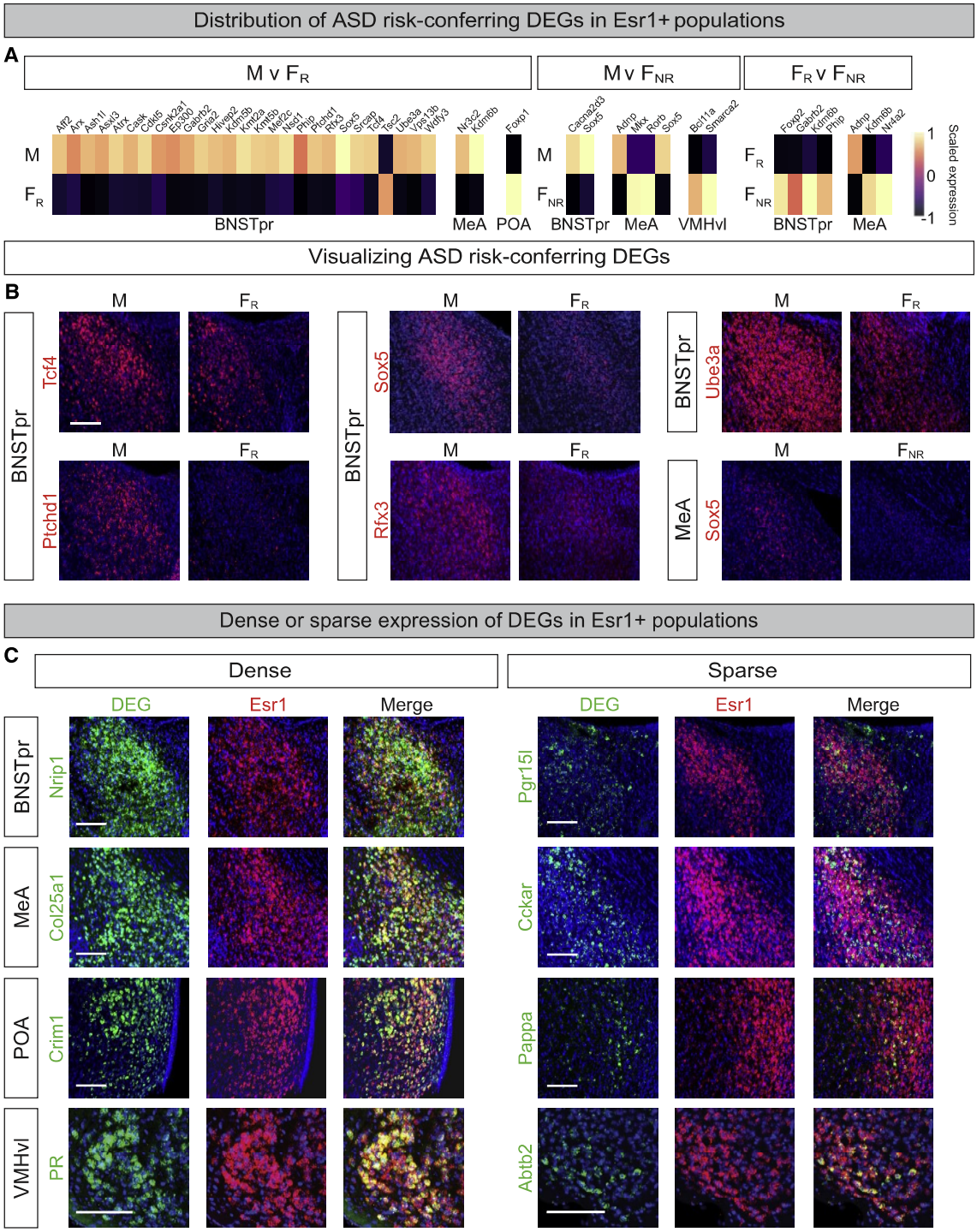

Figure 3. ASD association and distribution of DEGs *in vivo*

(A) Heatmap of expression of ASD risk-conferring DEGs. Scale = *Z*-scored expression of DEGs centered at zero for individual comparisons between conditions (sex or estrous state). See Figure 1C for heatmap and ISH for Auts2, an ASD-risk conferring DEG.

(B) ISH for ASD-risk conferring DEGs confirm TRAPseq data showing upregulation of Tcf4, Ptchd1, Sox5, Rfx3, and Ube3a in males. n = 2/condition/probe. Scale bar = 100 μm.

(C) ISHs for DEGs show that they are distributed in a few (sparse) or most (dense) Esr1^{+} neurons in each region. Quantification of these ISHs revealed that "sparse" and "dense" DEGs were expressed in $\leq$10% and $\geq$70% of Esr1^{+} cells. n = 2/condition/probe. Scale bar = 100 μm.

See also Figure S3.

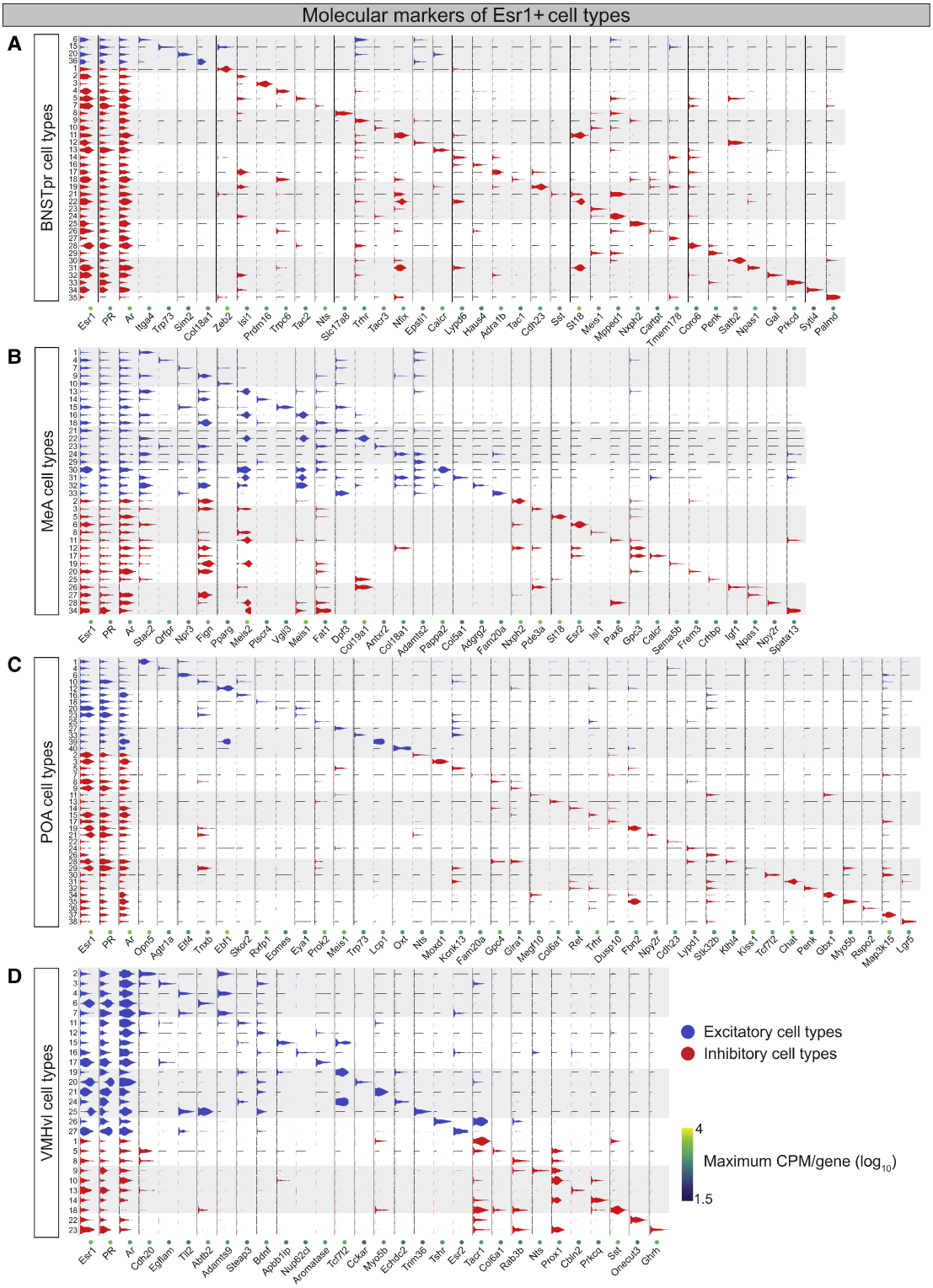

Figure 4. Categorizing Esr1$^+$ populations into cell types with snRNA-seq

Violin plots classifying Esr1$^+$ cell types (rows) by virtue of expression of sex hormone receptors, major neuronal neurotransmitter type (excitatory and inhibitory), and enriched genes in the BNSTpr (A), MeA (B), POA (C), and VMHvl (D). CPM, counts per million. n = 10,392 (BNSTpr), 15,929 (MeA), 17,784 (POA), and 5,671 (VMHvl) Esr1+ neurons.

See also Figure S4 and Tables S5 and S6.